

Interplay between theory and experiment in the quest for silica with reduced dimensionality grown on a Mo(1 1 2) surface

Marek Sierka^{a,*}, Tanya K. Todorova^a, Sarp Kaya^b, Dario Stacchiola^b,
Jonas Weissenrieder^b, Junling Lu^{b,c}, Hongjun Gao^c, Shamil Shaikhutdinov^b,
Hans-Joachim Freund^b, Joachim Sauer^a

^a *Humboldt-Universität zu Berlin, Institut für Chemie, Unter den Linden 6, 10099 Berlin, Germany*

^b *Fritz-Haber-Institut der Max-Planck-Gesellschaft, Faradayweg 4-6, 14195 Berlin, Germany*

^c *Institute of Physics, Chinese Academy of Sciences, P.O. Box 603, 100080 Beijing, China*

Received 10 April 2006

Available online 28 April 2006

Abstract

The stability of ordered one- and two-dimensional silica structures formed on a Mo(1 1 2) surface as a function of silicon coverage and oxygen pressure (phase diagram) is derived from density functional theory. At elevated oxygen pressures formation of a new, previously not considered structure of two-dimensional silica film is predicted. It contains additional oxygen atoms adsorbed directly on the Mo(1 1 2) surface underneath a two-dimensional network of corner sharing [SiO₄] tetrahedra. The existence of the new phase is confirmed experimentally using infrared reflection absorption spectroscopy and X-ray photoelectron spectroscopy.

© 2006 Elsevier B.V. All rights reserved.

Materials with reduced dimensionality receive continuously increasing interest because their properties may differ significantly from the properties of bulk materials. Particularly interesting are well-ordered thin oxide films grown on metal substrates which, apart from their applications in advanced technologies, can play an important role as models of otherwise very complex systems, e.g. oxide supported catalysts [1–4]. Such model systems allow investigations of structure–reactivity relationships on a molecular level [5,6]. Prerequisite is a detailed knowledge of structure and morphology of the thin oxide films under different ambient conditions, in particular oxygen partial pressures and temperatures. Despite tremendous progress in experimental techniques the determination of the atomic structure of thin films is possible only in combination with theoretical calculations [7–9].

Silica (SiO₂) remains one of the most widely used oxides in catalysis and advanced materials. Successful preparation

of a crystalline silica film on a Mo(1 1 2) substrate under ultrahigh vacuum (UHV) conditions was reported first by Schroeder et al. [10,11] and later by Goodman's group [12]. Combining density functional theory (DFT) and surface experiments, it has been shown that the film consists of a monolayer of two-dimensional (2D) network of corner sharing [SiO₄] tetrahedra [8,13]. Very recently, formation of one-dimensional (1D) silica structures (stripes) on the Mo(1 1 2) surface has been observed at low Si coverage [14]. DFT calculations demonstrated that these 1D stripes consist of paired rows of corner sharing [SiO₄] tetrahedra chemisorbed on the metal substrate. At increasing Si coverage, islands of the 2D film and stripes were found to coexist [14].

This unexpected variety of low dimensional silica phases formed under different conditions encouraged us to perform DFT calculations on ordered 1D and 2D silica structures on a Mo(1 1 2) surface and to combine the results in a phase diagram which shows their stability at different Si coverage and oxygen pressures. At elevated oxygen pressures the calculations predict formation of a new,

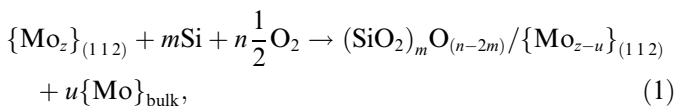
* Corresponding author. Fax: +49 30 2093 7136.

E-mail address: marek.sierka@chemie.hu-berlin.de (M. Sierka).

previously not considered structure of the 2D silica film. In addition to the network of corner sharing $[\text{SiO}_4]$ tetrahedra this structure contains oxygen atoms adsorbed directly on the Mo(112) surface. The existence of this new phase has been subsequently confirmed using infrared reflection absorption spectroscopy (IRAS) and X-ray photoelectron spectroscopy (XPS).

The present DFT calculations apply the same methodology as described before [8,13,14]. Briefly, the Vienna ab initio simulation package (VASP) [15,16] was used along with the Perdew–Wang (PW91) [17] exchange–correlation functional and the projector augmented wave (PAW) method [18,19]. The core-level energies including final state effects were calculated using a modified projector augmented wave method. Calculations of the vibrational spectra within the harmonic approximation used a central finite difference method with 0.02 Å displacements of the atoms in each Cartesian direction. The intensities were obtained from the derivatives of the dipole moment component perpendicular to the surface. To compensate for systematic errors of DFT we used an empirical scaling factor [20] of 1.0312, derived from the same type of calculations for α -quartz (see Supporting Information in Ref. [8]). The surface unit cell was modeled by slabs containing seven Mo layers with the four topmost fully relaxed.

To compare the stability of different $\text{SiO}_2/\text{Mo}(112)$ models we first define their formation energy, ΔE_{form} , from a clean Mo(112) surface, bulk silicon, and molecular oxygen:



where m and n are the number of Si and O atoms in the unit cell, respectively, and $(\text{SiO}_2)_m\text{O}_{(n-2m)}/\{\text{Mo}_{z-u}\}_{(112)}$ defines the composition of a particular $\text{SiO}_2/\text{Mo}(112)$ phase. The term $\{\text{Mo}\}_{\text{bulk}}$ appears for the missing-row reconstructed surfaces, which are assumed to be in equilibrium with bulk Mo. This reconstruction resulting in a change of Mo content in a unit cell is indicated by z and u . Since different models have different chemical composition, the values of ΔE_{form} cannot be used directly to compare the stability of the phases. Instead, we consider a surface related free energy change, $\Delta\gamma$, defined per surface area S

$$\Delta\gamma(T, p) = \frac{1}{S} [\Delta E_{\text{form}} - m\Delta\mu_{\text{Si}}(T, a_{\text{Si}}) - n\Delta\mu_{\text{O}}(T, p_{\text{O}_2})] \quad (2)$$

with $\Delta\mu_{\text{Si}}(T, a_{\text{Si}}) = \mu_{\text{Si}} - E_{\text{Si}}$ and $\Delta\mu_{\text{O}}(T, p_{\text{O}_2}) = \mu_{\text{O}} - 1/2E_{\text{O}_2}$, where μ_{Si} and μ_{O} are the silicon and oxygen chemical potentials, E_{Si} and E_{O_2} are energies of the bulk Si and molecular O_2 . The relative chemical potentials of Si and O, $\Delta\mu_{\text{Si}}(T, a_{\text{Si}})$ and $\Delta\mu_{\text{O}}(T, p_{\text{O}_2})$, respectively, can be related to silicon activity, a_{Si} , and oxygen partial pressure, p_{O_2} , using standard thermodynamics.

The experiments were performed in an UHV chamber (base pressure below 1×10^{-10} mbar) equipped with scanning tunneling microscopy (STM), XPS, an IR-spectrome-

ter and standard facilities for sample cleaning and preparation. The IR spectra were measured with a p-polarized light at 84° grazing angle of incidence (resolution $\sim 2 \text{ cm}^{-1}$). The binding energies (BE) in XPS spectra were calibrated relative to the Fermi edge of the clean Mo crystal. The preparation of the silica structures has been described in details elsewhere [8,13,14]. Briefly, a Mo(112) single crystal was cleaned prior to use via cycles of oxidation at elevated temperature and vacuum annealing at 2300 K. Various amounts of silicon (0.5–1.5 ML) were deposited in 5×10^{-8} mbar of O_2 onto the clean Mo(112) surface at 900 K, followed by annealing at 1100–1250 K either in UHV or 10^{-6} mbar O_2 (see below).

In search for the most stable structures comprising the phase diagram we have built more than 60 different models of 1D and 2D silica adsorbed on the Mo(112) surface with (1×2) , (1×3) , (2×2) , and (2×3) periodicities and different registries with respect to the substrate Mo atoms. For all the structures considered the most stable surface configuration (reconstructed vs unreconstructed) and distribution of surface oxygen atoms were found through our implementation of a genetic algorithm [21]. The advantage of this approach is that the number of atoms involved in the adsorption and reconstruction, as well as their most favorable bonding geometry under given conditions can be found automatically, without relying on intuition in interpreting the experimental data. The results of these calculations are presented in Fig. 1 as a two-dimensional phase diagram, which shows the stability regions of different silica phases as a function of $\Delta\mu_{\text{Si}}$ (i.e. amount of Si on the surface) and $\Delta\mu_{\text{O}}$ (i.e. oxygen partial pressure).

At low values of the chemical potentials the energetically most favorable structures are 1D silica stripes. At very reducing conditions ($\Delta\mu_{\text{O}} < -4 \text{ eV}$), the (1×3) stripes on clean, unreconstructed Mo(112) surface is the most stable model (S1, Fig. 1). Increasing oxygen pressure leads to adsorption of oxygen in pseudo threefold hollow sites on the protruding Mo rows running along the $[\bar{1}\bar{1}1]$ direction between the silica stripes. The adsorption occurs first on every second site in a ‘zigzag’ manner with a (2×3) periodicity, and then on all threefold hollow sites between the stripes leading to a (1×3) structure (S2 and S3, respectively, Fig. 1). Finally, at higher $\Delta\mu_{\text{O}}$ values ($\Delta\mu_{\text{O}} > -3.2 \text{ eV}$) the most stable model is 1D stripes separated by missing-row type reconstructed Mo(112) surface covered by oxygen atoms (S4, Fig. 1). Simulated STM images and calculated IRAS and XPS spectra for this structure were consistent with the experimental results [14]. Interestingly, this structure contains oxygen atoms adsorbed directly on the Mo surface underneath the silica stripes.

At high values of $\Delta\mu_{\text{Si}}$ and low values of $\Delta\mu_{\text{O}}$, the 2D crystalline silica film of corner sharing $[\text{SiO}_4]$ tetrahedra is formed, which corresponds to the structure 1 ML A reported in our previous publications [8,13]. However, for $\Delta\mu_{\text{O}} > -3.2 \text{ eV}$ a new phase denoted here as 1 ML $A/4\text{O}$ is predicted to be the most stable. It contains four addi-

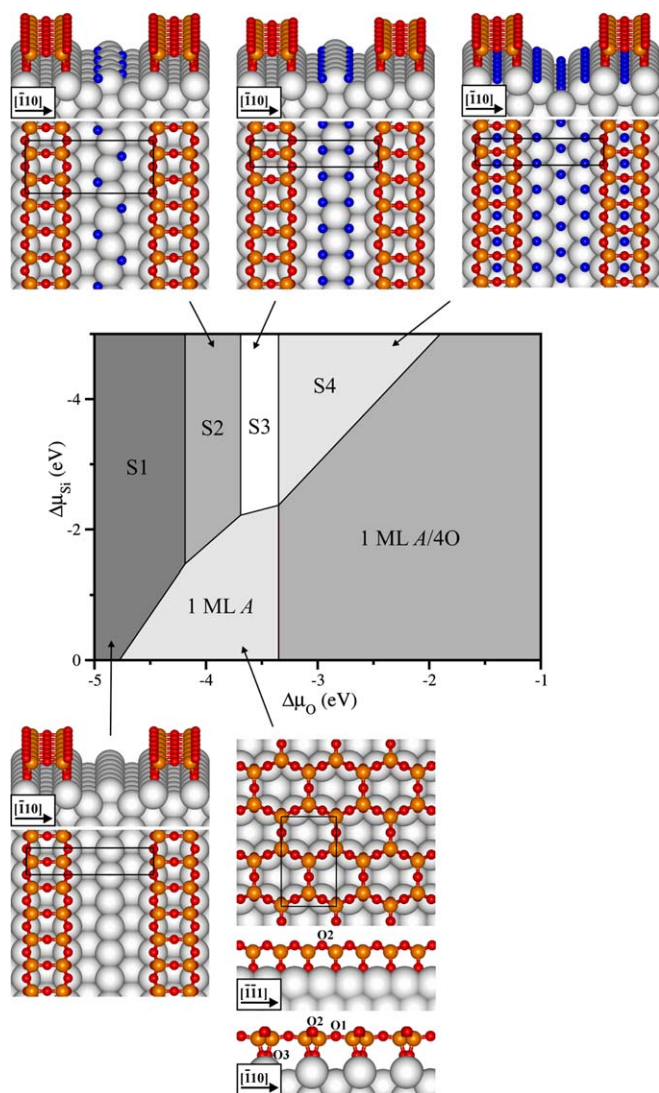


Fig. 1. Calculated phase diagram of 1D and 2D crystalline silica on a Mo(112) substrate as a function of $\Delta\mu_{\text{Si}}$ and $\Delta\mu_{\text{O}}$ chemical potentials. Oxygen atoms adsorbed on the Mo(112) surface (O^* species) are shown as blue spheres. The remaining O and Si atoms are represented by red and orange spheres, respectively. Surface unit cells are indicated as black rectangles. (For interpretation of the references to colour in this figure legend, the reader is referred to the web version of this article.)

tional oxygen atoms per surface unit cell, located in bridging position in the trenches of the Mo(112) surface along the $[\bar{1}\bar{1}1]$ direction (see Fig. 2). Models with one, two, and three additional oxygen atoms per unit cell were found less stable over the relevant range of $\Delta\mu_{\text{O}}$ (cf. Fig. 3). Adsorption of more than four oxygen atoms results in a subsurface oxidation of the Mo(112) substrate and a partial decomposition of the silica film. Comparison of structural parameters for the ‘oxygen-rich’ (1 ML A/4O) and the original ‘oxygen-poor’ (1 ML A) models shows that the additional oxygen atoms chemisorbed on the Mo surface have virtually no influence on the structure of the silica film. Thus, the properties of these two films are expected to be very similar.

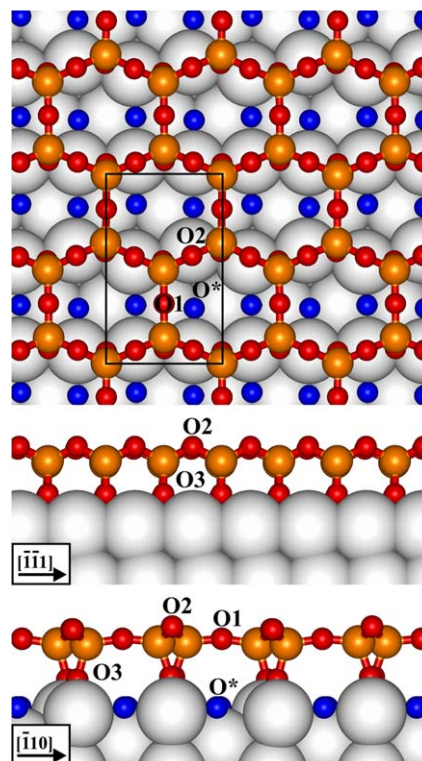


Fig. 2. Atomic structure of the O-rich (1 ML A/4O) phase of the 2D silica film on Mo(112). Oxygen atoms adsorbed on the Mo(112) surface (O^* species) are shown as blue spheres. The remaining O and Si atoms are represented by red and orange spheres, respectively. Surface unit cell is indicated as a black rectangle. (For interpretation of the references to colour in this figure legend, the reader is referred to the web version of this article.)

In order to distinguish these structures experimentally, the O-poor and O-rich silica films were prepared by annealing at 1250 K in UHV and in 10^{-6} mbar of O_2 , respectively. Both calculated and experimental STM images for the O-rich and O-poor films showed no discernable differences and were identical to those published previously [8,13]. Also no changes are observed in the LEED patterns, confirming that additional oxygen atoms chemisorbed on the Mo surface do not change a $c(2 \times 2)$ -Mo(112) symmetry. However, the analysis of vibrational properties and electronic structures using IRAS and XPS revealed substantial differences.

For the O-poor (1 ML A) film, the calculated IRAS spectrum showed a very intense band at 1061 cm^{-1} and two weak bands at 779 and 672 cm^{-1} as presented by the bars in Fig. 4. These bands were assigned to Si–O–Mo asymmetric stretching, Si–O–Si symmetric stretching coupled with Si–O–Si bending mode, and to a coupling of Si–O–Si bending modes [8,13], respectively, as schematically drawn as inset in Fig. 4. For the O-rich (1 ML A/4O) film, the calculated Si–O–Mo asymmetric stretching mode shifts to 1046 cm^{-1} , whereas positions of the two other bands remain virtually unchanged. In line with the theoretical predictions, the main peak in the experimental IRAS spectrum of the O-rich film is clearly red-shifted by

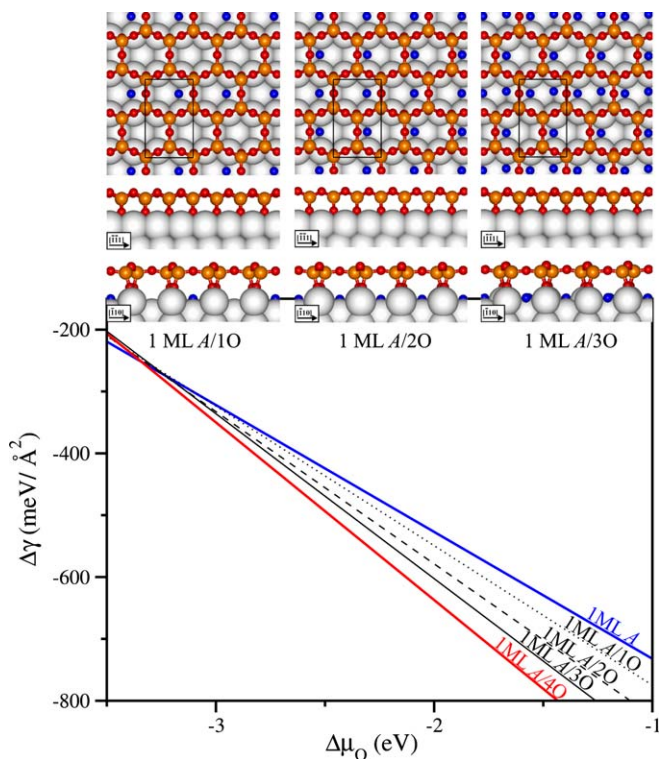


Fig. 3. Surface related free energy of formation $\Delta\gamma(T,p)$ as a function of oxygen chemical potential $\Delta\mu_{\text{O}}$ for the most stable 1 ML $A/n\text{O}$ models of the $\text{SiO}_2/\text{Mo}(112)$ film with additional n oxygen O^* atoms adsorbed directly on the $\text{Mo}(112)$ surface (shown as blue spheres). The 1 ML A and 1 ML $A/4\text{O}$ models are illustrated in Figs. 1 and 2, respectively. Surface unit cells are indicated as black rectangles. (For interpretation of the references to colour in this figure legend, the reader is referred to the web version of this article.)

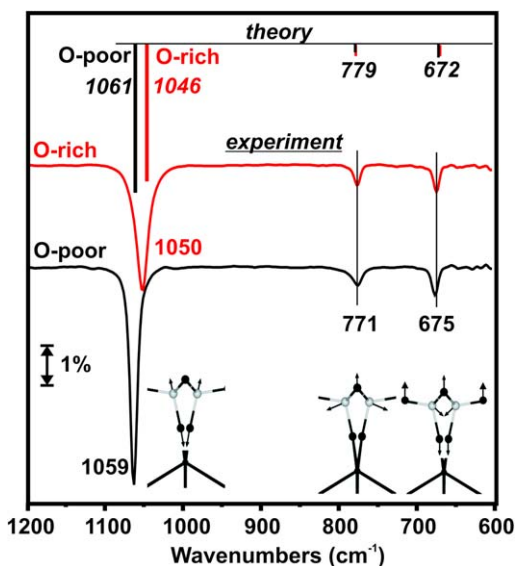


Fig. 4. IRAS spectra of the O-poor and O-rich silica films grown on $\text{Mo}(112)$. Calculated frequencies of the three IRAS most intense vibrations for 1 ML A and 1 ML $A/4\text{O}$ structures are represented by the bars with the height proportional to the intensity normal to the surface.

about 10 cm^{-1} with respect to the mode at 1059 cm^{-1} present in the O-poor film. As expected, no discernable differences are observed for the low-frequency vibrations at 771 and 675 cm^{-1} .

The results of XPS studies for these two films are summarized in Fig. 5. The experimental O 1s region of the XPS spectrum for the O-poor film shows two different oxygen species at 532.5 and 531.2 eV , assigned to the O atoms in the outermost layer (O1 and O2) and the interface O3 atoms bound to the Mo substrate, respectively [8,13]. The integral intensity ratio is 3:2 and the core-level shift of 1.3 eV is in perfect agreement with the calculated values [8,13]. For the O-rich film the presence of a third component centered 530.6 eV is clearly visible. Our calculations show, that this broad signal originates from O species chemisorbed on the $\text{Mo}(112)$ surface (marked as O^* in Fig. 2). These O^* atoms have virtually no influence on the BE of the oxygen atoms within the silica layer. However, they partially oxidize the surface Mo atoms, leading

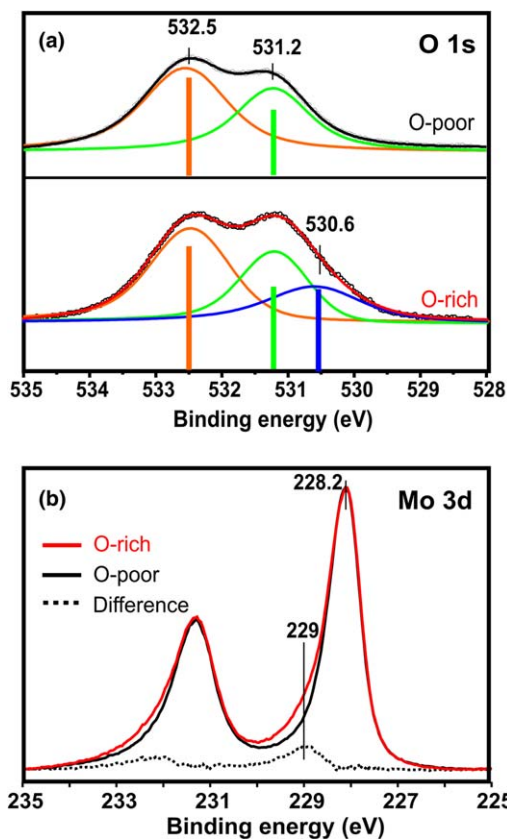


Fig. 5. The O 1s (a) and Mo 3d (b) regions of the XPS spectra of the O-rich and O-poor silica films formed on $\text{Mo}(112)$. Deconvolution of: (a) includes calculated core-level shift of 1.3 eV between $\text{O1}(\text{O2})$ and O3 atoms (see Fig. 1 for atoms labeling). The third component found for the O-rich film is assigned to O^* species present in the 1 ML $A/4\text{O}$ phase. The bars show BE values predicted by theory for the different O species in the model, with the height proportional to their number. The O^* species lead to partial oxidation of the surface Mo atoms resulting in the high BE shoulder of Mo 3d level as resolved in the difference spectrum on (b). Spectrum (b) is normalized with respect to intensity maximum of $\text{Mo } 3d_{5/2}$ to indicate the shoulder due to the extra oxygen atoms.

to the prominent shoulder at high BEs for the Mo 3d core level, which is even better resolved in the difference spectrum (see Fig. 5b). It is important to note that, once prepared the O-rich film cannot be converted back to the O-poor state. This is the consequence of a high binding energy of O* species to the Mo(112) surface, which has been estimated to 3.1–3.7 eV based on the present calculations. However, post-annealing of the O-poor film in oxygen ambient readily leads to the O-rich film.

In summary, we have demonstrated the predictive power of DFT in combination with genetic algorithm for structure determination. Our calculations not only resolved the atomic structure of experimentally observed phases of the SiO₂/Mo(112) system but also predicted formation of a new O-rich phase. Due to very subtle differences between properties of the O-poor and O-rich films, the existence of the latter might have not been discovered without the aid of theory. In addition, the observations of slightly different silica structures showing the same surface symmetry may shed light on the somewhat controversial results reported in the literature on silica films [10–12]. Since one of the main arguments in these discussions are the vibrational properties of the films, it appears that the experimental data may critically depend on the exact preparation procedure such as annealing temperature and whether annealing is performed in UHV or O₂ atmosphere. Even though the additional oxygen atoms chemisorbed on the Mo surface have little effect on the network structure of the silica film, these surface oxygen species formed at O₂ rich conditions should be taken into account in the reactions with metal ad-atoms deposited on the film (see e.g. Ref. [22]).

Acknowledgements

The authors gratefully acknowledge financial support by the Deutsche Forschungsgemeinschaft (DFG) and Fonds der Chemischen Industrie. T.K.T. and S.K. acknowledge the International Max Planck Research School ‘Complex Surfaces in Materials Science’ for a fellowship. D.S. and J.W. thank the Alexander von Humboldt Stiftung. The cal-

culations were carried out on the IBM p690 system of the Norddeutscher Verbund für Hoch- und Höchstleistungsrechnen (HLRN).

References

- [1] S.A. Chambers, Surf. Sci. Rep. 39 (2000) 105.
- [2] H.L. Meyerheim, R. Popesco, J. Kirschner, N. Jedrecy, M. Sauvage-Simkin, B. Heinrich, R. Pinchaux, Phys. Rev. Lett. 87 (2001) 076102.
- [3] S. Schintke, S. Messerli, M. Pivetta, F. Patthey, L. Libioulle, M. Stengel, A. De Vita, W.-D. Schneider, Phys. Rev. Lett. 87 (2001) 276801.
- [4] Y.T. Matulevich, T.J. Vink, P.A. Zeijlman van Emmichoven, Phys. Rev. Lett. 89 (2002) 167601.
- [5] D.R. Rainer, D.W. Goodman, J. Molec. Catal. A: Chemical 131 (1998) 259.
- [6] H.-J. Freund, Surf. Sci. 500 (2002) 271.
- [7] G. Kresse, M. Schmid, E. Napetschnig, M. Shishkin, L. Köhler, P. Varga, Science 308 (2005) 1440.
- [8] J. Weissenrieder, S. Kaya, J.-L. Lu, H.-J. Gao, S. Shaikhutdinov, H.-J. Freund, M. Sierka, T.K. Todorova, J. Sauer, Phys. Rev. Lett. 95 (2005) 076103.
- [9] L. Giordano, D. Ricci, G. Pacchioni, P. Ugliengo, Surf. Sci. 584 (2005) 225.
- [10] T. Schroeder, M. Adelt, B. Richter, M. Naschitzki, M. Bäumer, H.-J. Freund, Surf. Rev. Lett. 7 (2000) 7.
- [11] T. Schroeder, J.B. Giorgi, M. Bäumer, H.-J. Freund, Phys. Rev. B 66 (2002) 165422.
- [12] M.S. Chen, A.K. Santra, D.W. Goodman, Phys. Rev. B 69 (2004) 155404.
- [13] T.K. Todorova, M. Sierka, J. Sauer, S. Kaya, J. Weissenrieder, J.-L. Lu, H.-J. Gao, S. Shaikhutdinov, H.-J. Freund, Phys. Rev. B 73 (2006) 165404.
- [14] J.-L. Lu, S. Kaya, J. Weissenrieder, T. K. Todorova, M. Sierka, J. Sauer, H.-J. Gao, S. Shaikhutdinov, H.-J. Freund, Surf. Sci. Lett. (in press).
- [15] G. Kresse, J. Furthmüller, Comput. Mater. Sci. 6 (1996) 15.
- [16] G. Kresse, J. Furthmüller, Phys. Rev. B 54 (1996) 11169.
- [17] J.P. Perdew, J.A. Chevary, S.H. Vosko, K.A. Jackson, M.R. Pederson, D.J. Singh, C. Fiolhais, Phys. Rev. B 46 (1992) 6671.
- [18] P.E. Blöchl, Phys. Rev. B 50 (1994) 17953.
- [19] G. Kresse, D. Joubert, Phys. Rev. B 59 (1999) 1758.
- [20] A.P. Scott, L. Radom, J. Phys. Chem. 100 (1996) 16502.
- [21] M. Sierka, T. K. Todorova, to be published.
- [22] L. Giordano, A. Del Vitto, G. Pacchioni, J. Chem. Phys. 124 (2006) 034701.